Spectral Signature of Magnetic Flux Tubes in Sunspot Penumbrae

D.A.N. Müller, R. Schlichenmaier, O. Steiner & M. Stix
Kiepenheuer-Institut für Sonnenphysik, Freiburg, Germany

Abstract

We investigate the polarization of spectral lines in the penumbra of sunspots by integrating the radiative transfer equation of polarized light for a three-dimensional axially symmetric model atmosphere of a sunspot. The Evershed flow is confined to horizontal magnetic flux tubes, which are embedded in an inclined magnetic field. We compute the net circular polarization (NCP), $N = \int V(\lambda) d\lambda$, of the two photospheric spectral lines Fe I 630.25 nm and Fe I 1564.8 nm. Analyzing spectra at a fixed distance from the spot center, we find that the azimuthal variation, $N(\psi)$, is an antisymmetric function of ψ with respect to the line connecting disk center and spot center for Fe I 1564.8 nm, while the variation is predominantly symmetric for Fe I 630.25 nm. We show that the antisymmetric variation is caused by anomalous dispersion.

A Sunspot Model

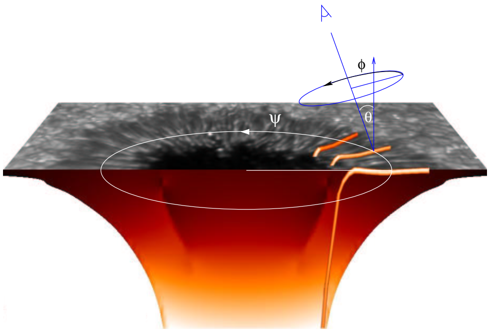

Magnetic flux tubes in the penumbra. The azimuthal angle ϕ and the inclination γ of the magnetic field vary with the location of the flux tube in the sunspot.

- Tripartite magnetostatic sunspot model (Jahn & Schmidt 1994)
- Moving flux tube model (Schlichenmaier et al. 1998):
  - heat transport: mixing length theory
  - heat exchange at the magnetopause
  - concept of interchange convection
- Three-dimensional representation & radiative transfer module SPOTMACHINE (Müller et al. 2002)

Vertical cut through the penumbra:

- Background: axisymmetric vector field
- Field-aligned flow inside flux tube

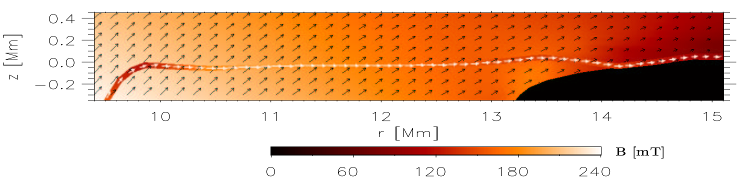

Asymmetric Stokes-V Profiles

Pictorial Representation of the Stokes Parameters

$I = \updownarrow + \leftrightarrow, \quad Q = \updownarrow - \leftrightarrow, \quad U = \nwarrow - \nearrow, \quad V = \circlearrowright - \circlearrowleft$

Stokes-V Profiles

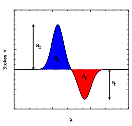

Net Circular Polarization (NCP)
$\mathcal{N} \equiv \int V d\lambda = A_b - A_r$

- Velocity gradients are necessary *and* sufficent to produce NCP
- NCP independent of macroturbulence / instrumental broadening

Asymmetries: $\mathcal{N} \equiv \int V d\lambda \neq 0 \quad \Leftrightarrow \quad \frac{\partial v(\tau)}{\partial \tau} \neq 0$

Radiative Transfer Equation for Polarized Light

$$\frac{d}{ds}\begin{pmatrix} I \\ Q \\ U \\ V \end{pmatrix} = -\begin{pmatrix} \eta_I & \eta_Q & \eta_U & \eta_V \\ \eta_Q & \eta_I & \rho_V & -\rho_U \\ \eta_U & -\rho_V & \eta_I & \rho_Q \\ \eta_V & \rho_U & -\rho_Q & \eta_I \end{pmatrix}\begin{pmatrix} I \\ Q \\ U \\ V \end{pmatrix} + \begin{pmatrix} j_I \\ j_Q \\ j_U \\ j_V \end{pmatrix}$$

η_I:	Absorption	→ absorption coefficient for unpolarized light
$\eta_Q,\ \eta_U,\ \eta_V$:	Dichroism	→ the absorption properties of the medium depend on the polarization of radiation
$\rho_Q,\ \rho_U,\ \rho_V$:	Anomalous Dispersion	→ the velocity of propagation of the wave in the medium depends on its polarization state

Doppler Shift vs. Zeeman Splitting

Doppler Shift: $\Delta\lambda_D \propto \lambda$, Zeeman Splitting: $\Delta\lambda_Z \propto \lambda^2$

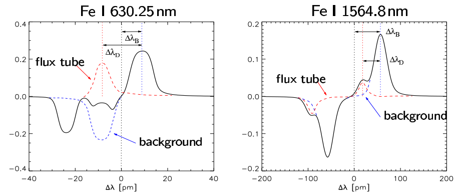

$\Delta\lambda_D > \Delta\lambda_Z$ $\Delta\lambda_D < \Delta\lambda_Z$

Breaking the Symmetry: Azimuthal Jump

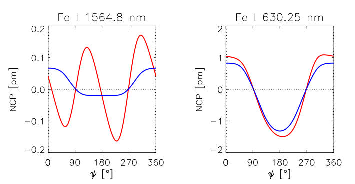

NCP, $N(\psi)$, along an azimuthal section

blue lines: *without* anomalous dispersion

red lines: *with* anomalous dispersion

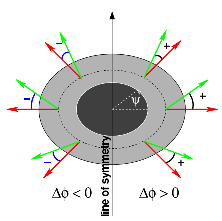

Analytical Model:
Single discontinuity along the line-of-sight (Landolfi & Landi Degl'Innocenti 1996):

- $\mathcal{N}_{\Delta\phi} \neq 0 \Leftrightarrow$ anomalous dispersion included!
- $\mathcal{N}_{\Delta\phi} \propto \sin(2\cdot\Delta\phi)$, i.e. antisymmetric
- $\mathcal{N}_{\Delta\gamma}$ symmetric

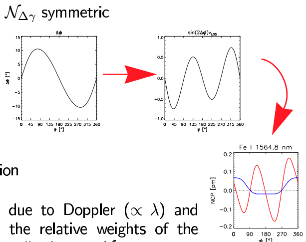

⇒ $\Delta\phi$ antisymmetric, while $\Delta\gamma$ & Δv symmetric

⇒ $\mathcal{N}(\psi)$ = symmetric contribution from $\Delta\gamma$ − effect
+ antisymmetric contribution from $\Delta\phi$ − effect

⇒ The ratio of wavelength shifts due to Doppler ($\propto \lambda$) and Zeeman effect ($\propto \lambda^2$) determines the relative weights of the symmetric and the antisymmetric contributions to $\mathcal{N}$.

Synthetic NCP-Maps & Comparison With Observations

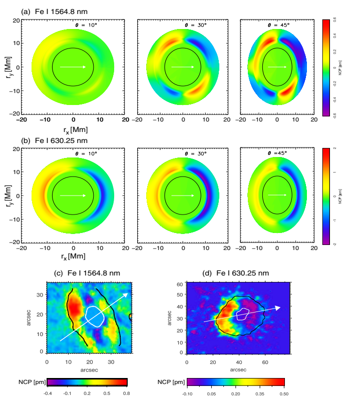

Synthetic NCP maps for Fe I 1564.8 nm (a) and Fe I 630.25 nm (b) for different heliocentric angles, θ. The black lines mark the umbral boundary, the arrows point towards disk center. Observations: (c) with the Tenerife Infrared Polarimeter, *(d) with the* Advanced Stokes Polarimeter *(courtesy V. Martínez Pillet).*

Azimuthal Variation of NCP:

- *symmetric* for Fe I 630.25 nm
- *antisymmetric* for Fe I 1564.8 nm

Radial Variation of NCP:

- NCP declines outwards as Δγ decreases

Center-to-limb Variation of NCP:

- Fe I 630.25 nm: *decrease* for large heliocentric angles
- Fe I 1564.8 nm: *increase* of NCP up to θ = 60°

Conclusions

- Observed NCP distribution can be reproduced by uncombed magnetic fields
- **Symmetry breaking by anomalous dispersion is essential to understand observations**
- Multi-line analysis facilitates discrimination between atmospheric configurations
- Synthetic Stokes maps can be used to retrieve physical quantities of the penumbra (Stokes inversion)

References

Jahn, K. & Schmidt, H. U. 1994, A&A, 290, 295
Landolfi, M. & Landi Degl'Innocenti, E. 1996, Sol. Phys.,164,191
Schlichenmaier, R., Jahn, K., & Schmidt, H. U. 1998, A&A , 337, 897
Schlichenmaier, R., Müller, D.A.N., Steiner, O. & Stix, M. 2002, A&A, 381, L77
Müller, D.A.N., Schlichenmaier, R., Steiner, O. & Stix, M. 2002, A&A, submitted